BRAIN
ORIGINAL ARTICLE

Brainstem pathology in anti-IgLON5 disease: new insights into early events and tau progression

Raphael Reinecke,[1,2] Sophie Nitsch,[1,2] Francisca Faber,[1,2] Cansu Elmas,[1,2] Marlene Gaubinger,[1,2] Anika Simonovska Serra,[1,2] Verena Endmayr,[1,2] Inga Koneczny,[1,2] Evelyn Berger-Sieczkowski,[2,3] Morten Blaabjerg,[4] M. Elena Erro,[5] Julia Ferrari,[6] Markus Glatzel,[7] Anna Heidbreder,[8] Birgit Högl,[9] Casper Jansen,[10] Jan Lewerenz,[11] Patrizia Moser,[12] Liisa Myllykangas,[13] Jeanette Krogh Petersen,[14] Peter Schnider,[15] Ambra Stefani,[9] Maarten J. Titulaer,[16] Deniz Yilmazer-Hanke,[17] Serge Weis,[18] Lidia Sabater,[19] Carles Gaig,[20] Ellen Gelpi[1,2,†] and Romana Höftberger[1,2,†]

[†]These authors contributed equally to this work.

Anti-IgLON5 disease is a rare neurological disease at the intersection of autoimmunity and neurodegeneration. It is characterized by the presence of anti-IgLON5 antibodies and the development of a brainstem-dominant tau pathology. Recent research indicates that the tau pathology may develop in a time-dependent manner. A three-staged neuropathological classification of the disease has been recently suggested, ranging from no or minimal tau (stage 1) to the characteristic brainstem tau pathology (stage 3) as originally described. This study aimed to characterize the evolution of the disease-associated tauopathy more precisely and to further investigate the early neurodegenerative events in anti-IgLON5 disease.

We analysed the medullary region of 14 autopsy cases of anti-IgLON5 disease with different severity grades of tau pathology and varying disease durations, from 6 to 180 months, and compared our findings with five cases with progressive supranuclear palsy and 10 neurologically healthy controls by immunohistochemistry. We applied a broad panel of antibodies targeting different pathological tau post-translational modification sites and the nuclear membrane. In addition, we performed a cell culture of rat hippocampal neurons incubated with purified anti-IgLON5 antibodies to validate the results of the autopsy samples.

Based on the tau burden in relation to the pathology stage and disease duration, we determined the chronological appearance of the different post-translational modifications of tau. Phosphorylation at serine 422 was identified as one of the first alterations at stage 1 and showed an early neuronal nuclear staining with simultaneous anti-IgLON5 IgG4 deposits on the neuronal surface as observed by double immunolabelling. Nuclear membrane alterations were also evident by Lamin B1 staining. These were significantly more frequent at stage 1 as compared with controls and adopted the form of nuclear invaginations and crenellations. Crenellations of the nuclear membrane also developed in neuronal cell culture after 3 weeks of antibody incubation, supporting the autopsy findings *in vitro*.

The development of cytoplasmic tau pathology occurs at later stages of the disease with a sequence of post-translational modifications, after an initial nuclear pathology. These new findings contribute to a better understanding of the early pathophysiological events in anti-IgLON5 disease and reinforce the concept of a secondary tauopathy related to an immune-mediated mechanism.

Received July 14, 2025. Revised November 05, 2025. Accepted December 11, 2025. Advance access publication January 17, 2026

1 Division of Neuropathology and Neurochemistry, Department of Neurology, Medical University of Vienna, Vienna 1090, Austria
2 Comprehensive Center for Clinical Neurosciences and Mental Health Vienna, Medical University of Vienna, Vienna 1090, Austria
3 Department of Neurology, Medical University of Vienna, Austria, Vienna 1090, Austria
4 Department of Neurology, Odense University Hospital, Odense C DK-5000, Denmark
5 Neurology Department, Hospital Universitario de Navarra, Health Research Institute of Navarra (IdisNA), Pamplona 31008, Spain
6 Department of Neurology, Hospital Barmherzige Brüder Vienna, Vienna 1020, Austria
7 Institute of Neuropathology, University Medical Center Hamburg-Eppendorf, Hamburg 20251, Germany
8 Department of Neurology, Kepler University Hospital Linz, Linz 4021, Austria
9 Department of Neurology, Medical University of Innsbruck, Innsbruck 6020, Austria
10 Laboratory of Pathology Eastern Netherlands, BB Hengelo 7555, The Netherlands
11 Department of Neurology, University Hospital Ulm, Ulm 89081, Germany
12 Department of Neuropathology, University Hospital Innsbruck, Innsbruck 6020, Austria
13 Department of Pathology, University of Helsinki and HUS Diagnostic Center, Helsinki University Hospital, Helsinki 00014, Finland
14 Department of Pathology, Odense University Hospital, Odense C DK-5000, Denmark
15 Clinical Department of Neurology, University Hospital Wiener Neustadt, NÖ Landesgesundheitsagentur – Danube Private University, Wiener Neustadt 2700, Austria
16 Department of Neurology, Erasmus University Medical Center, Rotterdam 3015 GD, The Netherlands
17 Clinical Neuroanatomy, Department of Neurology, University Hospital Ulm, Ulm 89081, Germany
18 Division of Neuropathology, Department of Pathology and Molecular Pathology, Kepler University Hospital and Clinical Research Institute for Neuroscience, Johannes Kepler University, Linz 4021, Austria
19 Neuroimmunology Program, Fundació de Recerca Clínic Barcelona-Institut d'Investigacions Biomèdiques August Pi i Sunyer, Universitat de Barcelona, Barcelona 08036, Spain
20 Department of Neurology, Hospital Clínic, Barcelona 08036, Spain

Correspondence to: Romana Höftberger
Division of Neuropathology and Neurochemistry, Department of Neurology, Währinger Gürtel 18–20, Vienna 1090, Austria
E-mail: romana.hoeftberger@meduniwien.ac.at

Keywords: autoimmune encephalitis; neurodegeneration; tauopathy; secondary tauopathy; nuclear alterations

Introduction

Anti-IgLON5 disease is a rare neurological disease at the intersection of autoimmunity and neurodegeneration. Since the discovery of the disease-associated anti-IgLON5 antibodies in patients with a peculiar type of sleep disorder 10 years ago, intensive work has been carried out to decipher the disease mechanisms, which are still not fully understood.[1,2] Bulbar symptoms were described as the most common initial clinical presentation, followed by REM and non-REM sleep disturbances, movement abnormalities reminiscent of progressive supranuclear palsy (PSP) as well as cognitive impairment.[3] During the disease course, most patients develop a combination of these symptoms, including other brainstem symptoms and autonomic dysfunction. The clinical spectrum of the disease makes early diagnosis difficult, which is further complicated by the fact that a delayed initiation of treatment is also associated with a poor prognosis and high mortality.[3] Consistent with the symptoms observed in affected patients, a brainstem- and hypothalamus-dominant neurodegeneration with a novel type of tauopathy was identified in an initial autopsy cohort study, leading to the first neuropathological classification of the disease in 2016.[4] Over time, however, there were cases identified without or only minimal tau deposits at autopsy.[5,6]

To account for the new findings, an updated neuropathological classification was developed in 2024 in an autopsy cohort of 22 cases and suggested a time-dependent three-stage pathology model: stage 1 with mild neurodegeneration and no or only minimal tau pathology; stage 2 with moderate neurodegeneration and mild to moderate tauopathy; and stage 3 with prominent neurodegeneration and tauopathy, corresponding to the characteristic tauopathy originally described.[1,7] Moreover, stage 1 was supported by the identification of IgG4 deposits in the brainstem and cerebellum in a fraction of the cases.[6] Patients at stage 1 had a higher age at initial manifestation and a short disease duration of less than 2 years, while patients at stage 3 had an earlier age of onset but a significantly longer disease duration of up to 6 years. The precise mechanisms behind the shorter disease course in older patients are currently unknown. However, a reduced 'brain resilience' of the elderly brain, for example due to co-pathologies, could play a role, making it more susceptible to the functional effects of the antibodies.[7]

The hypothesis that the tauopathy is a time-dependent phenomenon and that anti-IgLON5 disease represents a primary autoimmune disease that induces a secondary tauopathy is supported by other recent studies. For example, a pathogenic effect of IgG1 and IgG4 subclasses of the anti-IgLON5 antibody has been demonstrated *in vitro*.[8-10] In addition, it has been shown that patients with anti-IgLON5 disease show a strong HLA association, particularly with HLA-DQB1*05 subtypes,[11] and new data show that an early

start of therapy is associated with a better clinical outcome.[12,13] However, the exact mechanism by which antibody binding leads to the development of tauopathy remains unclear.

From a neuropathological point of view, there is a need for additional markers at the early stage of pathology, in particular in cases with no or only minimal tau pathology (stage 1) of patients who had neurological symptoms and anti-IgLON5 antibodies in blood and/or CSF. In addition, an exact characterization of the pathological post-translational modifications (PTM) of the tau protein and their sequential occurrence during pathology progression is lacking for anti-IgLON5 disease.

The objective of this study was therefore to characterize the evolution of the disease-associated tauopathy more precisely, to further investigate the early steps of neurodegeneration in an effort to identify new diagnostic markers and to provide new insights into the pathophysiology of anti-IgLON5 disease.

Materials and methods

Autopsy cohort

For this study, we included a total of 14 brain autopsies of patients with anti-IgLON5 disease, with a representative number of each disease stage 1–3. Cases from the previous study,[7] for which sufficient material was available for the study question, were used (for details, see Table 1). All cases had clinical symptoms and neuropathological findings consistent with anti-IgLON5 disease; 13/14 cases had positive anti-IgLON5 antibodies in the CSF. In one case (Case 8), antibody determination was no longer possible in the post-mortem stage. Brains were collected at different centres throughout Europe, including Austria ($n = 5$), Germany ($n = 3$), Finland ($n = 2$), Spain ($n = 1$), the Netherlands ($n = 1$), Slovenia ($n = 1$) and Denmark ($n = 1$). Clinical information on the initial subtype was taken from the structured questionnaires already collected for the previous study.[7]

In addition, we included 10 age-matched controls without known neurological disease as well as five cases with PSP as a 'tauopathy' positive control, four of which tested negative for anti-IgLON5 antibodies in the CSF. In one case (Case 17), testing was not possible as the CSF or serum was no longer available, but the patient presented clinically with a classical PSP phenotype without any atypical findings [see Supplementary Table 1, available at doi.org/10.5281/zenodo.17486565, Cases 15–21 for part I ($n = 7$) of the study and Cases 15–29 for part II ($n = 15$)]. Since previous studies showed that the lower brainstem is one of the first regions affected by neurodegeneration in anti-IgLON5 disease, leading to neurological symptoms, and this region is routinely sampled in the diagnostic workup, we used exclusively samples of the medulla oblongata for this study. Ethical approval for the use of post-mortem brain tissue for research studies was obtained from the Medical University of Vienna (EK 1123/2015 and 1636/2019).

Antibodies for the characterization of the tauopathy: part I

For immunohistochemical (IHC) analyses, we used 13 different antibodies directed to different pathological PTMs of the tau protein. The selection of antibodies was based on those available and already established for other tauopathies. A full list of antibodies with name, target epitope, manufacturer and pre-treatment conditions can be found in Table 2. Immunohistochemical staining on 5-μm thick, formalin-fixed, paraffin-embedded tissue sections was performed on an autostainer Link48 (Dako) for the antibodies AT8, RD3 and RD4 tau isoforms. The remaining antibodies were applied manually according to an in-house protocol with the tissue section pretreatments as listed in Table 2. Image acquisition was performed using a NanoZoomer S20MD digital slide scanner (Hamamatsu Photonics) and a Nikon Eclipse Ni-E microscope (Nikon).

Assessment and quantification of tau pathology

Depending on the individual section and exact level of the medulla oblongata, the following core areas were examined, as far as present on the tissue section: dorsal motor nucleus of the vagal nerve, hypoglossal nucleus, solitary tract and nucleus, nucleus ambiguus, gigantocellular nuclei/reticular formation and inferior olives. The burden of tau pathology was assessed in anti-IgLON5 cases ($n = 14$), PSP ($n = 5$) and controls ($n = 2$) semi-quantitatively, separately for each pretangles, tangles, threads, nuclear staining and glial tau pathology at the area of maximum disease burden in the above-mentioned regions as previously performed,[7] as follows: 0 = absent, i = isolated (<3 tau-positive neuropil threads/<1 pretangle/tangle/nucleus/glial tau); 1 = mild (3–15 positive neuropil threads, >2 pretangles and <5 tangles/nuclei/glial tau); 2 = moderate (>15 positive neuropil threads, >3 pretangles and >5 tangles/nuclei/glial tau); 3 = abundant (abundant neuropil threads and >10 pretangles/tangles/nuclei/glial tau). Based on the intensity of tau pathology in relation to the stage and the duration of the disease, a timeline was created with the approximate occurrence of the pathological steps over the course of the disease.

Evaluation of early pathological events at the cellular level: part II

For the investigation of early pathological events at the cellular level, we focused on the analysis of the nuclear morphology. For this, we used an antibody targeting Lamin B1 (Table 2) for visualizing the nuclear membrane. For the quantification of nuclear membrane changes, we assessed all clearly recognizable neurons with a fully depicted nucleus in a predefined area of the medulla oblongata that included the above-mentioned neuroanatomical areas. Nuclear invaginations and crenellations of 14 anti-IgLON5 disease cases, five PSP cases and 10 controls were categorized semi-quantitatively into 'normal', 'mild', 'moderate' and 'severe'. For nuclear invaginations, 'mild' corresponded to a membrane infolding of less than one-third of the nuclear diameter, 'moderate' to more than one-third of the diameter and 'severe' to multiple and almost cross-nuclear infoldings. For statistical analysis, normal/mild and moderate/severe were grouped and then compared. With regard to nuclear crenellations, 'mild' corresponded to an early splitting of the membrane, 'moderate' to the development of multiple indentations and 'severe' to a shrivelling of the nucleus. For statistical analysis, 'normal', 'mild/moderate' and 'severe' were compared among controls, PSP and anti-IgLON5 disease 'total' as well as along the different stages of pathology (stages 1 to 3). The changes were assessed blinded to condition and stages. Owing to the limited number of samples, statistical analyses were performed using the Kruskal–Wallis test followed by Dunn's multiple comparison test. This was done for comparing controls and PSP to all IgLON5 cases as a whole as well as to individual IgLON5 stages. The calculations and visualization of the data were performed using Prism 10 (Version 10.4.2).

To examine the spatial relationship between tau and anti-IgLON5 antibodies in the early pathology stages, we performed

Table 1 Demographic and clinical data of anti-IgLON5 disease autopsy cases

Case	Stage	Sex	Age at onset	Age at death	Disease duration (months)	Clinical symptoms at onset	Cause of death	HLA type	Immunotherapy	IgG-subclasses: IgG1/IgG2/ IgG3/IgG4 (in %)
1	1	Male	81	82	6	Bulbar syndrome, sleep disorder	Pneumonia, sepsis	DRB1*10:01, DQB1*05:01, DRB1*15:01, DQB1*06:02	IVIg, RTX	n/a
2	1	Male	77	77	9	Bulbar syndrome, PSP-like syndrome	n/a	DRB1*08:01/DRB1*10:01, DQB1*04:02/ DQB1*05:01	None	n/a
3	1	Male	81	82	11	Movement disorder, cognitive impairment	Respiratory insufficiency (unknown cause)	n/a	IVMP	n/a
4	1	Male	71	73	24	Sleep disorder, PSP-like syndrome	Sudden death (unknown cause)	DRB1*10:01;DQB1*05:01	IVIg	n/a
5	2	Male	75[a]	76	6[a]	PSP-like syndrome, cognitive impairment	n/a	n/a	IVMP, oral steroids, MMF	n/a
6	2	Male	66	72	96	PSP-like syndrome	Respiratory failure	DRB1*10:01; DQB1*05:01	IVMP, oral steroids, RTX	n/a
7	2	Male	62	75	156	PSP-like syndrome	Pneumonia, status epilepticus	DRB1*03:01/DRB1*14:01 DQB1*05:03/ DQB1*02:01	None	11.1/1.1/0.5/87.2
8	3	Female	66	71	60	Bulbar syndrome	Infection of unknown origin	n/a	None	n/a
9	3	Female	70	76	72	Bulbar syndrome, sleep disorder	Respiratory failure	DRB1*01:01, DRB1*11:01, DQB1*03:01, DQB1*05:01, DQA1*01:01, DQA1*05:05	IVMP, IVIg, PLEX, RTX	n/a
10	3	Male	67	76	108	PSP-like syndrome, bulbar syndrome	Subdural haematoma	DRB1*01:02, DRB1*03:01; DQB1*02:01, DQB1*05:01	None	20/0/0/79.9
11	3	Female	61	70	108	PSP-like syndrome	Pneumonia	DRB1*01:01/DRB1*04:04, DQB1*05:01/ DQB1*03:02	IVIg	n/a
12	3	Female	77	87	120	Bulbar syndrome	Sudden while asleep	n/a	None	n/a
13	3	Female	54	66	156	Sleep disorder, bulbar syndrome	Aspiration pneumonia	DRB1*10:01; DQB1*05:01	None	36.5/1.6/0/61.7
14	3	Male	50	65	180	Bulbar syndrome, sleep disorder	Respiratory failures	DRB1*10:01; DQB1*05:01	IVMP, PLEX, RTX	n/a

All anti-IgLON5 cases were included in the previous study by Gelpi *et al.*,[7] the table is adapted from that study accordingly. n/a = not available; IVMP = intravenous methylprednisolone; IVIg = intravenous immunoglobulins; MMF = mycophenolate mofetil; PLEX = plasmapheresis; PSP = progressive supranuclear palsy; RTX = rituximab.

[a]Minimum disease duration, exact time of symptom onset not known; IgG subclasses: first sample (from disease onset) is indicated.

Table 2 Antibodies and target epitopes

Antibody	Epitope	Host (clone)	Source/identifier	Pretreatment/dilution
Tau antibodies				
AT8	Phosphorylation at Ser202/Thr205	Mouse (AT8)	Thermo Scientific/Cat. No. MN1020	None/1:200
3RD	3-repeat tau isoform	Mouse (8E6/C11)	Millipore, Sigma Aldrich/Cat. No. 05-803	Citrate buffer pH 6 + 1 min FA/1:2000
4RD	4-repeat tau isoform	Mouse (1E1/A6)	Millipore, Sigma Aldrich/Cat. No. 05-804	Citrate buffer pH 6 + 1 min FA/1:800
AT100	Phosphorylation at Thr212/Ser214	Mouse (AT100)	Thermo Scientific/Cat. No. MN1060	None/1:500
AT180	Phosphorylation at Thr231	Mouse (AT180)	Thermo Scientific/Cat. No. MN1040	Citrate buffer pH 6/1:500
AT270	Phosphorylation at Thr181	Mouse (AT270)	Thermo Scientific/Cat. No. MN1050	None/1:1000
Alz-50	Misfolded conformation of tau (aa 2–10 and 312–342)	Mouse	Gift from Peter Davis Lab	Citrate buffer pH 6/ 1:160[a]
MC1	Misfolded conformation of tau (aa 2–10 and 312–342) without cross-reactivity for FAC1	Mouse	Gift from Peter Davis Lab	Citrate buffer pH 6/1:80[a]
PHF-1	Phosphorylation at Ser396/Ser404	Mouse	Gift from Peter Davis Lab	Citrate buffer pH 6/ 1:160[a]
pTau Ser356	Phosphorylation at Ser356	Rabbit	Affinity Bioscience/Cat. No. AF3143	Citrate buffer pH 6/ 1:2000
pTau Ser262	Phosphorylation at Ser262	Rabbit	Affinity Bioscience/Cat. No. AF3151	Citrate buffer pH 6/1:200
pTau Ser422	Phosphorylation at Ser422	Rabbit	Affinity Bioscience/Cat. No. AF3145	Citrate buffer pH 6/1:200
Ac-Tau K274	Acetylation at K274	Rabbit (MAB359)	Gift from Li Gan Lab	Citrate buffer pH 6 + 1 min FA/1:1000
Other antibodies				
IgG4		Mouse (HP6025)	Bio-Rad/Cat. No. MCA2098G	EDTA pH 9/1:500
Lamin B1		Rabbit	Abcam/Cat. No. ab16048	EDTA pH 9/1:1000
CD8		Mouse (C8/144B)	Dako/Cat. No. M7103	Citrate buffer pH 6/1:100
Granzyme B		Rabbit	Cell Marque/Cat. No. EP230	EDTA pH 9/1:50
MHC-I		Mouse	Gift from Hans Lassmann	EDTA pH 9/1:2000

Antibodies used in this study for immunohistochemistry and immunofluorescence and their respective target epitope as well as source and identifier when applicable. aa = amino acid; FA = formic acid; FAC1 = fetal Alz-50-reactive clone 1.
[a]Antibodies received as supernatant.

double immunolabelling for light microscopy with anti-IgG4 and anti-pTS422 antibodies in representative cases at stage 1 (Casess 1 and 4). For quantitative analyses, we assessed the area with maximal IgG4 deposits and counted all neurons within two adjacent square millimetres and categorized them as IgG4 positive (deposits along the neuronal membrane), pTS422 nuclear positive, double positive and double negative. One representative case from stage 2 (Case 7) and stage 3 (Case 11) was used as a control. Chromogenic reactions with two different substrates, Fast Blue (blue) and 3-amino-9-ethylcarbazole (AEC; PolyDetector Liquid AEC HRP Red, BioSB), were used for double labelling of different antigens.

Evaluation of CD8+ T-cell density in anti-IgLON5 disease and PSP

To assess the contribution of cellular cytotoxicity in both diseases, we performed anti-CD8 immunostaining in all cases with available material (anti-IgLON5 disease, $n = 12$; PSP, $n = 4$). Quantification was performed using an ocular morphometric grid to measure the number of parenchymal and perivascular T cells per 1 mm^2 in the area of maximal inflammation, as previously described.[6] In representative cases with the highest CD8+ T-cell burden from each stage of anti-IgLON5 disease and PSP (Cases 4, 7, 13 and 16), we also performed immunostaining for Granzyme B, MHC-I and a double immunolabelling with anti-CD8 and anti-pTS422 to evaluate the spatial relationship of cytotoxic T cells and pTS422-positive neurons.

Isolation of anti-IgLON5 IgG antibodies and subclass purification

Plasmapheresis material from an anti-IgLON5 disease patient with clinically bulbar as well as PSP-like symptoms and serum from a healthy donor were diluted 1:4 in PBS, filtered using 0.2 µm filters, and incubated overnight at 4°C with gentle rolling with Pierce Protein A/G Plus Agarose (Thermo Scientific, Cat. No. 20423) for total IgG isolation. For IgG4 isolation, the total IgG in

PBS was applied directly to a column containing CaptureSelect IgG4 (Hu) Affinity Matrix (Thermo Scientific, Cat. No. 2942902005). The column flow-through was subsequently applied to a column containing CaptureSelect IgG1 (Hu) Affinity Matrix (Thermo Scientific, Cat. No. 191303005) to isolate IgG1. All affinity matrices were packed into 1.5 mm diameter columns (Bio-Rad, Cat. No. 7371507) and washed with PBS. Bound IgG was eluted in 1 ml fractions using 0.1 M glycine (pH 2.3) and immediately neutralized with 1 M Tris base (pH 8.0). Protein concentrations were determined by absorbance at 280 nm, and the fractions with the highest concentrations were pooled and dialysed to PBS using Spectra-Por Float-A-Lyzer G2 (Sigma-Aldrich, Cat. No. Z727253) according to the manufacturer's instructions. The analysis of IgG subclasses was adapted from previously described methods.[13] In short, HEK293 cells were transfected with full-length human IgLON5 fused to TurboGFP. Transfected cells were incubated with purified IgG from patient serum, followed by subclass-specific mouse anti-human antibodies (IgG1–4) and anti-mouse IgG conjugated with Cy3 for detection. Flow cytometry was used to measure the median

fluorescence intensity (MFI) of Cy3 in the phycoerythrin (PE) channel. To correct for non-specific binding, ΔMFI values were calculated by subtracting the MFI of $tGFP^-$ cells from that of $tGFP^+$ cells. This assay was independently repeated three times. The final composition of the patients' total IgG showed a percentage distribution of 17.5% IgG1, 2.7% IgG2 and 79.8% IgG4. IgG1 purification yielded a result of an IgG1 fraction of 100%, and IgG4 purification yielded an IgG4 fraction of 85.9% and 6.5% of IgG1 (6.8% IgG2 and 0.7% IgG3).

Rat hippocampal neuronal cell culture

Rat hippocampal neuronal cell cultures were carried out from embryonic Day 18 embryos as previously described.[14] On Day 7, treatment with purified healthy control IgG, anti-IgLON5 IgG total, as well as purified IgG1 and IgG4 antibody subclasses (as detailed earlier) was initiated at a final concentration of 10 µg/ml, based on prior studies with anti-IgLON5 antibody incubation.[8] Treatment was refreshed weekly with the addition of 1 ml of antibody-containing medium per 35 mm culture dish. A treatment-naive control group received only medium without antibody incubation. After 3 weeks of antibody incubation, neurons were stained live with human serum from a patient with anti-IgLON5 disease. In addition, cultures were stained with anti-Lamin B1 (1:500, Abcam, Cat. No. ab16048), neurofilament protein (NFP; 1:400, Dako, Clone 2F11) and pTau422 (1:100, Affinity Bioscience, Cat. No. AF3145) antibodies after fixation with paraformaldehyde, followed by anti-human, anti-rabbit and anti-mouse IgG Alexa Fluor 488 (1:1000, Jackson ImmunoResearch, Lot#129707/139784/155613), respectively. The experiments were repeated four times independently. Confocal microscope images were captured using an Olympus BX63 microscope (Olympus) with a numerical aperture of 1.40 for the 40× and 100× objectives. Since all secondary antibodies were conjugated with Alexa Flour 488, fluorescence was recorded using the corresponding FITC filter set (excitation wavelength 494 nm, emission wavelength 518 nm). Nuclei were stained with DAPI (DAPI filter, excitation wavelength 345 nm, emission wavelength 455 nm). The quantification of nuclear changes in the form of crenellations was performed semi-quantitatively, analogous to histology. For the quantification, the nuclei of all neurons present on the coverslips were analysed. The percentage of moderately and severely crenellated nuclei was evaluated for the individual experiments, and the mean value was calculated for each condition. Statistical analysis between groups was performed using the Kruskal–Wallis test followed by Dunn's multiple comparison test. Quantification studies were done by investigators blinded to the condition. The calculations and visualization of the data were performed using Prism 10 (Version 10.4.2).

Results

Detailed characterization of the tau pathology and timeline of pathologic steps in anti-IgLON5 disease

According to the previously published staging system based on the AT8 antibody, which targets the Ser202/Thr205 phosphorylation sites of tau, cases at stage 3 had the highest tau pathology load, cases at stage 2 had an intermediate load and cases in stage 1 had no or only minimal tau. However, when applying other antibodies targeting different PTM sites, we observed different patterns, particularly with regard to the intensity of tau burden in the different pathology stages [see Fig. 1 for an example illustration of five representative antibodies along the three stages, ranging from the earliest to the latest pathological step, and Supplementary Fig. 1 (available at doi.org/10.5281/zenodo.17486565) for the remaining antibodies examined and a comparison with PSP and controls].

Based on the intensity of tau burden, in relation to the stage and disease duration, we determined the chronological appearance of the different pathological steps of tau pathology as follows (earliest to latest): phosphorylation at Ser422 (pTauS422), phosphorylation at Ser202/Thr205 (AT8), phosphorylation at Thr231 (AT180), phosphorylation at Ser396/Ser404 (PHF-1), misfolded conformation of tau aa 2–10 and 312–342 (Alz50/MC1), phosphorylation at Thr212/Ser214 (AT100), 4-repeat tau (RD4), phosphorylation at Ser356 (pTauSer356), phosphorylation at Ser262 (pTauSer262), 3-repeat tau (RD3), acetylation at K274 (ac-Tau) and phosphorylation at Thr181 (AT270). The full scores and antibody results are presented in Supplementary Table 2 (available at doi.org/10.5281/zenodo.17486565). While most of these post-translational modifications occurred at stage 2, pTauS422 showed a positive staining in all stage 1 cases with at least isolated threads and more intense staining in two cases, while RD3 tau staining, ac-Tau and AT270 only occurred at stage 3. We mapped the pathologic steps of the tau pathology along the different disease stages in a schematic timeline, which is depicted in Fig. 2, and included our previously described neuropathological data on the IgG4 immunolabelling.[6] The immunohistochemical profile of the different tau phosphorylation steps, however, did not clearly differ from the PSP cases used as a positive control for an established brainstem-dominant tauopathy. These results indicate that the neuronal tau pathology associated with anti-IgLON5 disease currently cannot be neuropathologically differentiated from the tau pathology related to PSP based solely on this anti-tau antibody profile. The only exception is the presence of 3R tau isoforms in the late disease stages of anti-IgLON5 disease (see Table 3 for a comparison of the PTM profiles of anti-IgLON5 disease with the other well-characterized tauopathies). The neurologically healthy controls showed almost completely negative results, confirming the specificity of the antibodies for tau pathology.

As previously reported, we detected a variable amount of glial tau in most anti-IgLON5 disease autopsies. This was particularly evident in the form of oligodendroglial tau with coiled bodies in mild to moderate severity. However, individual cases also showed thorn-shaped astrocytes. The glial tau pathology developed similarly to the neuronal component over time, but in comparison showed increased immunolabelling with the antibodies PHF-1, RD4 and ac-Tau (Supplementary Table 2).

Nuclear tau appears before cytoplasmic tau and relates to IgG4 deposits

Previous descriptions of the tau pathology of anti-IgLON5 disease are based on immunostainings with AT8, RD3 and RD4 antibodies, and mainly revealed the cytoplasmic component of tau in the form of pretangles, tangles and threads. This was particularly evident in the AT8 staining in cases with moderate and advanced pathology (stages 2 and 3), but not in early stages (stage 1). In this study, we identified a positive pTauS422 staining in neuronal nuclei in a fraction of cases at stage 1. This pattern was not only observed at stage 1 but also in some stage 2 and stage 3 cases and was often associated with an irregular nuclear membrane morphology (Fig. 3A).

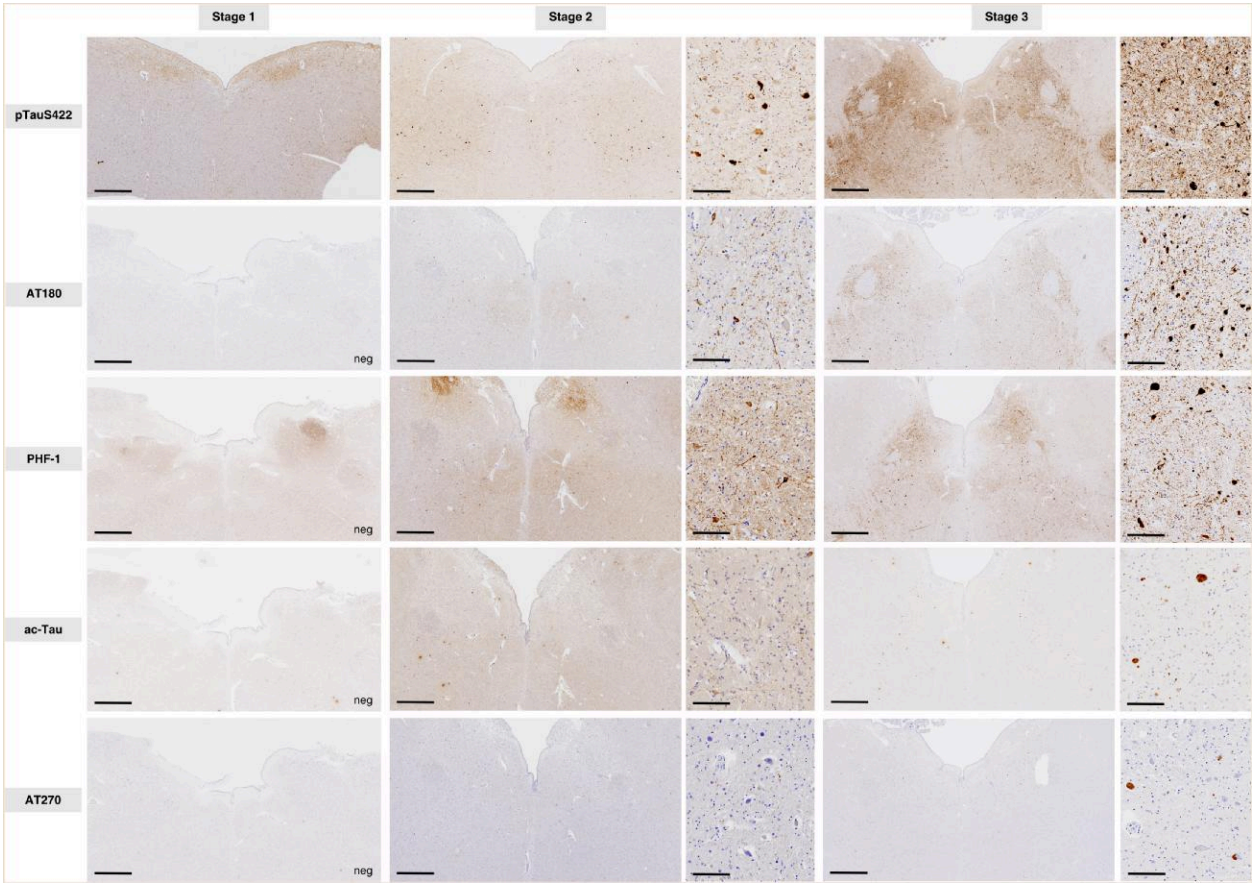

Figure 1 Development of the tauopathy in the medulla oblongata during the course of anti-IgLON5 disease. Based on five example antibodies, ranging from a first phosphorylation step at Ser422 (pTauSer422) to a late step at Thr181 (AT270), a progressive increase in tau pathology can be seen from stages 1 to 3. In parallel, there is a decrease in tau pathology from the early to the late phosphorylation steps within one stage. The same case is shown for all antibodies for each stage, respectively, with the exception of Ser422 in stages 1 and 2, to demonstrate the early staining pattern. The depicted areas include one or more of the following areas, depending on the sampling-related level: dorsal motor nucleus of the vagal nerve, hypoglossal nucleus, solitary tract and nucleus, nucleus ambiguus, raphe nuclei. Neg = negative staining. Scale bars = 800 µm, *insets* in stages 2 and 3 = 45 µm. Stage 1 = Case 2 (pTS422 Case 1), stage 2 = Case 5 (pTS422 Case 7), stage 3 = Case 13.

Additionally, cases at stage 2 and stage 3 also had higher pTauS422 load compared with AT8, suggesting that phosphorylation at Ser422, in combination with early nuclear changes, is an earlier event than phosphorylation at Ser202/Thr205 (AT8) and thus one of the first alterations detectable by IHC in anti-IgLON5 disease. Nuclear staining was also seen with the AT100 antibody, as well as occasionally with pTS356 and ac-Tau (K274) antibodies. In a singular PSP case, nuclear tau was only mildly seen by AT100 staining, while in the controls, only very isolated neurons showed nuclear staining.

In accordance with the immunohistochemical timeline of post-translational tau modifications (Fig. 2), the early nuclear changes observed with pTS422 co-occurred in areas with IgG4 deposits in two patients at stage 1, who died of brainstem symptoms but showed no obvious tau deposits applying the AT8 antibody. In both cases, double immunostaining showed several neurons framed by IgG4 deposits that were previously shown to correspond to anti-IgLON5 antibodies.[6] A total of 7.8% of the neurons in the areas with maximal IgG4 deposits showed concomitant membranous IgG4 and nuclear staining for pTauS422, indicating both a temporal and spatial relationship between antibody deposition and early nuclear tau accumulation [Fig. 3B and Supplementary Fig. 2A (available at doi.org/10.5281/zenodo.17486565)]. This association was not observed in example stage 2 and stage 3 cases, where only pTS422 but not membranous IgG4 staining was detected (Supplementary Fig. 2B and C).

The CD8+ T-cell component does not differ between anti-IgLON5 disease and PSP

Our previous study showed a similar amount of T cells in the parenchymal and perivascular compartments between anti-IgLON5 disease and PSP.[6] To assess whether the cellular inflammatory component could also play a relevant role in the development of the tauopathy along the different stages of anti-IgLON5 disease, or whether this could be used to distinguish it from PSP, we also performed immunostaining for CD8, Granzyme B and MHC-I. Quantification of CD8+ T cells revealed no significant differences in parenchymal or perivascular compartments along the three disease stages or in comparison to PSP, although in line with previous findings,[6] parenchymal CD8+ T cells were less pronounced in PSP [Supplementary Fig. 3A (available at doi.org/10.5281/zenodo.17486565)]. In isolated cases, particularly in stage 1, CD8+ T cells were found in the immediate proximity of or adjacent to neurons (Supplementary Fig. 3B). Only isolated Granzyme B+ T cells were found in the vicinity of neurons (Supplementary Fig. 3C). MHC-I was strongly expressed in microglia, other nucleated cells and

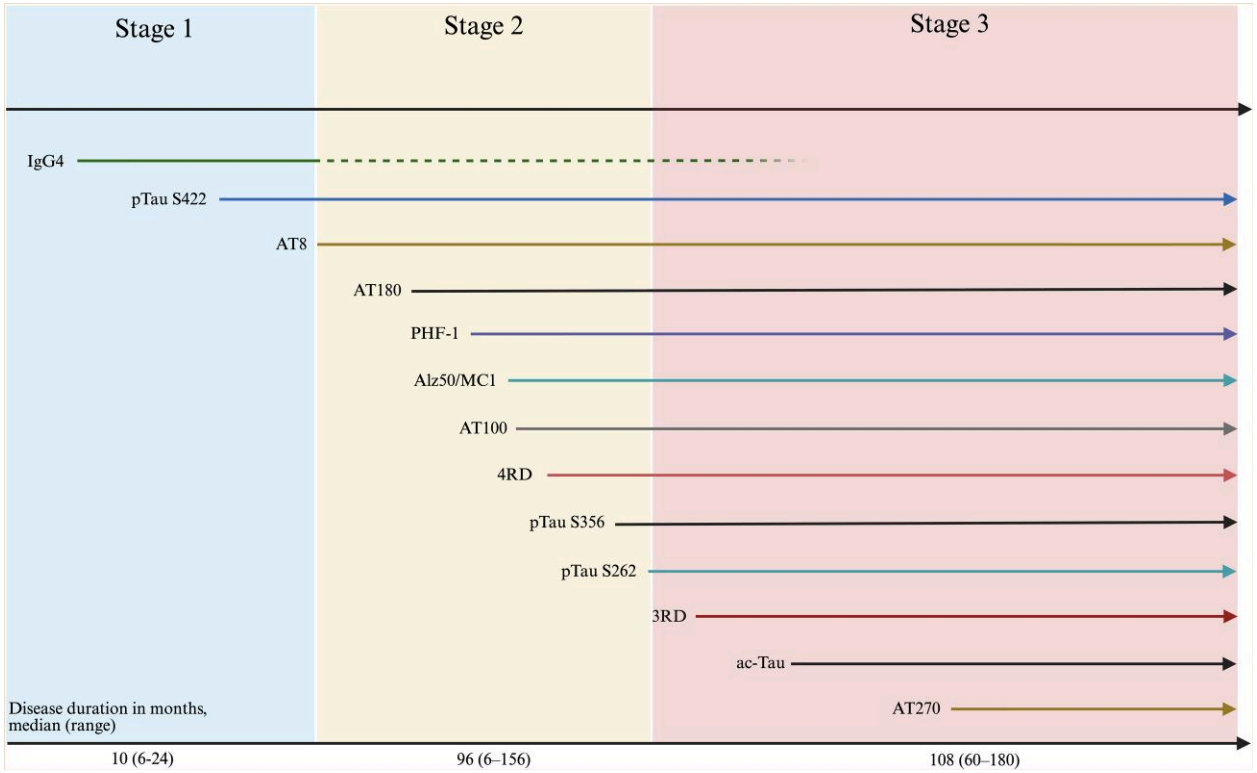

Figure 2 Schematic timeline representation of the tau pathology and IgG4 in anti-IgLON5 disease. While IgG4 predominates in stage 1, only pTauS422 appears during this stage. Most post-translational modifications occur at stage 2, while singular ones only occur at stage 3. The dashed line in IgG4 indicates that IgG4 depositions were still detectable in individual cases of stages 2 and 3, but in fewer regions and in significantly lower quantities than in stage 1 cases. The order of appearance is based on the corresponding detectability at the different disease stages and the disease duration. Created in BioRender. Höftberger, R. (2026) https://BioRender.com/agutm6l.

Table 3 Comparison of phosphorylated and acetylated epitopes of tau protein in anti-IgLON5 disease and other tauopathies

Antibody	Phosphorylation/acetylation sites	3R + 4R 4R > 3R Anti-IgLON5 Own	3R + 4R AD Lit[15]	3R + 4R CTE Lit[16,17]	4R PSP Own	4R PSP Lit[18-20]	3R PiD Lit[18,21-23]	4R AGD Lit[24-26]
AT8	Ser202/Thr205	+	+	+	+	+	+	+
3RD	3-repeat tau	+	+	+	–	–	+	–
4RD	4-repeat tau	+	+	+	+	+	–	+
AT100	Thr212/Ser214	+	+	+	+	+	+	+
AT180	Thr231	+	+	+	+	+	+	+
AT270	Thr181	+	+	?	+	?	+	+
Alz-50	aa 2–10 and 312–342	+	+	?	+	+	+	+
PHF-1	Ser396/Ser404	+	+	+	+	+	+	+
pTau Ser356	Ser356	+	+	?	+	?	–	–
pTau Ser262	Ser262	+	+	+	+	?	–	–
pTau Ser422	Ser422	+	+	+	+	+	+	+
Ac-Tau K274[27]	Acetylation at K274	+	+	+	+	+	+	–

Phosphorylated/acetylated sites in the respective tauopathies are indicated with '+', if not present, sites are indicated with '–'; ? = no data in literature; own = results from the present study; Lit = results from literature review; 3R = 3-repeat tau isoforms; 4R = 4-repeat tau isoforms; aa 2–10 and 312–342 = misfolded conformation of tau at amino acids 2–10 and 312–342; AD = Alzheimer's disease; AGD = argyrophilic grain disease; CTE = chronic traumatic encephalopathy; PiD = Pick's disease; PSP = progressive supranuclear palsy.

vessels, with increased intensity in cases with more severe pathology. A fraction of neuronal perikarya was also immunolabelled in cases and areas with more severe pathology (data not shown). In contrast to IgG4, we could not identify CD8+ T cells abutting to neurons with nuclear pTS422 staining by double immunohistochemistry in anti-IgLON5 disease (Supplementary Fig. 3D).

Alterations of the morphology of the nuclear membrane represent an early sign of neurodegeneration in anti-IgLON5 disease

Based on our findings of early tau phosphorylation at S422 in a nuclear distribution and the identification of nuclear membrane alterations, we immunolabelled the nuclear membrane with

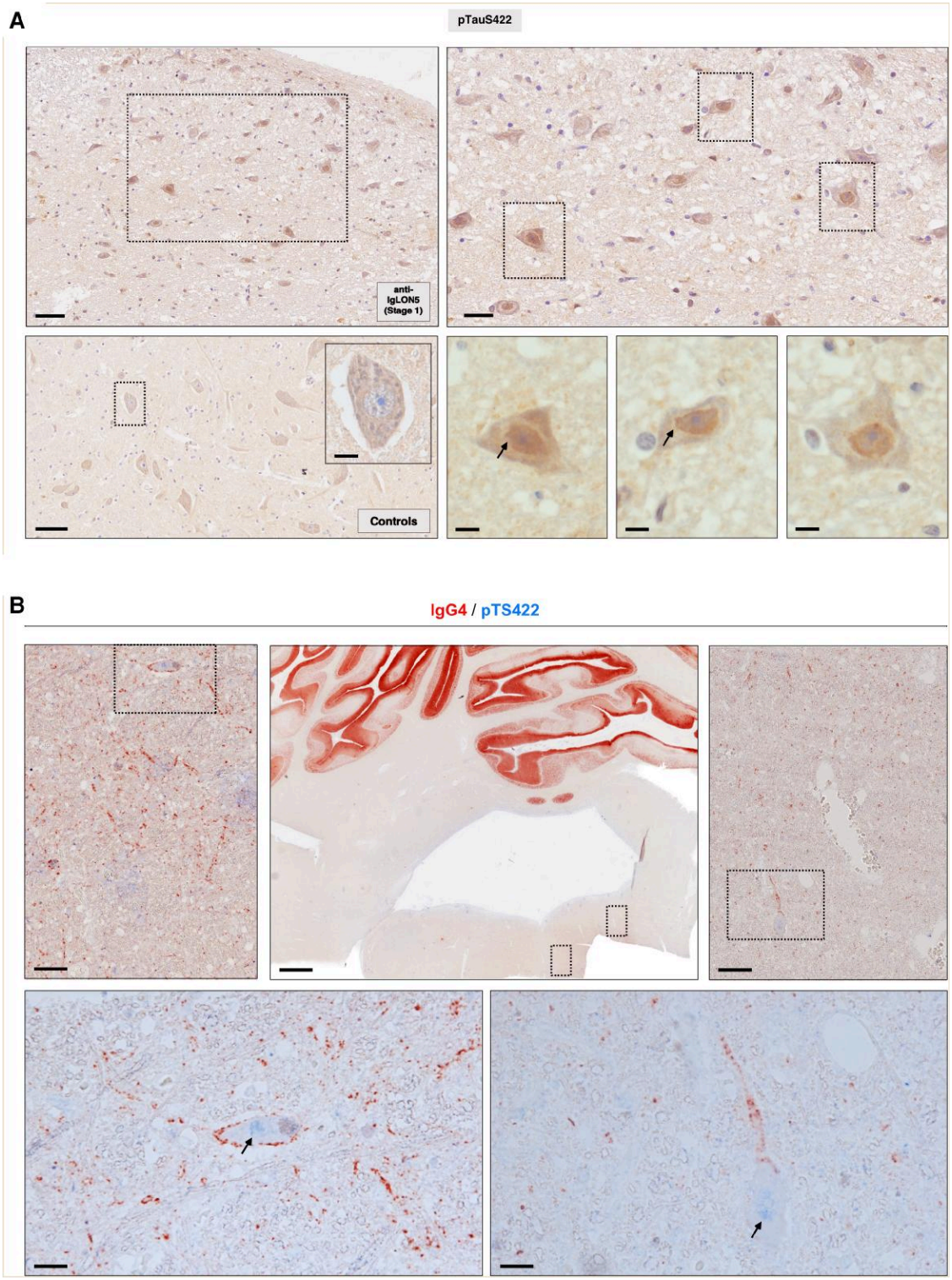

Figure 3 Nuclear staining pattern of pTauS422 and co-distribution with anti-IgLON5 antibodies. (**A**) Staining for pTauS422 revealed a nuclear staining pattern in stage 1 cases, which was not evident in control cases (*bottom left*). Higher magnification (*top right* and *bottom right*) additionally revealed irregular borders of the nuclear membrane in the IgLON5 cases (arrows in *insets*). Scale bars = 250 µm (*top left*); 100 µm (*top right* and *bottom left*); 5 µm (*bottom right* and *bottom left inset*). Stage 1 = Case 4, control = Case 20. (**B**) Double immunostaining with anti-IgG4 (red, corresponding to anti-IgLON5 antibodies) and anti-pTauS422 (blue) antibodies in stage 1 cases reveals simultaneous deposition of anti-IgLON5 IgG4 antibodies along the neuronal surface and nuclear pTauS422 staining (arrows in *bottom row*) in multiple neurons, Case 1. Note that the stainings in **A** and **B** have different secondary detection systems, resulting in nuclear staining patterns that are not completely identical. Scale bars = 2.5 mm (*top middle*); 50 µm (*top left* and *right*); 15 µm (*bottom row*).

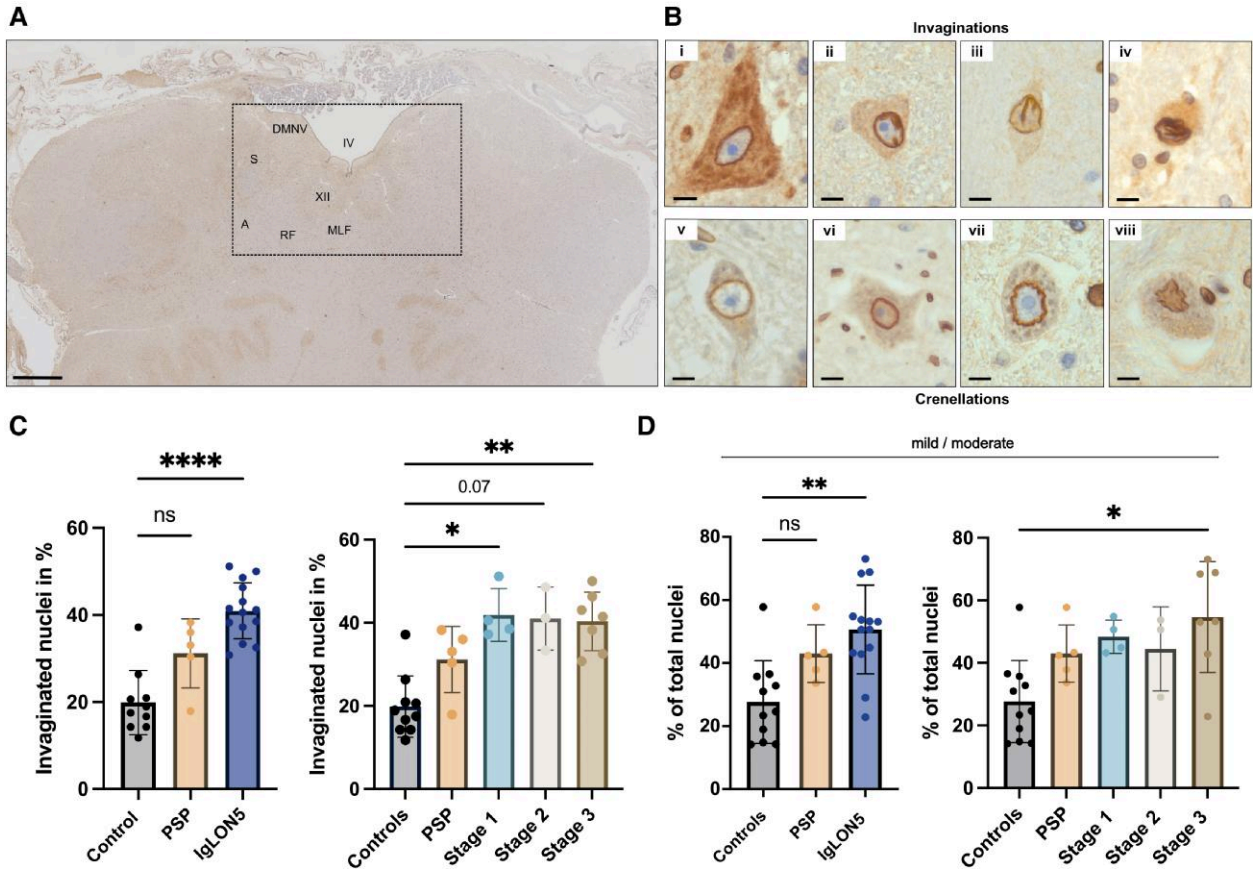

Figure 4 Nuclear membrane alterations in anti-IgLON5 disease. (**A** and **B**) **Anti-Lamin B1 immunohistochemistry.** (**A**) All neurons in the depicted area, including hypoglossal nucleus (XII), dorsal motor nucleus of the vagal nerve (DMNV), the solitary nucleus (S), nucleus ambiguus (A) and reticular formation, were analysed. (**B**) Exampe images for invaginations ranging from (**i**) a normal nuclear membrane morphology to (**ii**) mild (less than one-third of nuclear diameter), (**iii**) moderate (more than one-third of nuclear diameter) and (**iv**) severe invaginations. Crenellations were also graded as (**v**) normal, (**vi**) mild, (**vii**) moderate and (**viii**) severe crenellations. (**C** and **D**) Statistical analysis. Percentage of invaginations (**C**) and mild/moderate crenellations (**D**) comparing controls to all anti-IgLON5 disease cases as well as to different disease stages separately, $^{*}P < 0.05$, $^{**}P < 0.01$, $^{***}P < 0.001$, $^{****}P < 0.0001$. IV = fourth ventricle, MLF = medial longitudinal fasciculus. Scale bars = 2.5 mm (**A**), 5 µm (**B**).

antibodies directed against Lamin B1 and compared the anti-IgLON5 disease cohort with PSP cases and age-matched controls without neurological disease in the area of maximal disease severity in the medulla oblongata (Fig. 4A). Here, we observed two main types of changes of the nuclear membrane: nuclear invaginations and nuclear crenellations.

Nuclear invaginations were characterized by infoldings of the membrane to different degrees into the nucleus [Fig. 4B(i–iv)]. If defined as less than one-third of the nuclear diameter (moderate/severe), a significantly higher percentage of invaginated neurons was found when all anti-IgLON5 disease cases were compared with controls (40.9% versus 19.9%, $P < 0.0001$; Fig. 4C). The mild increase in invaginations in PSP compared with controls (mean difference: 11.3%, $P = 0.452$) and in anti-IgLON5 disease compared with PSP (mean difference 9.7%, $P = 0.183$) did not reach significance. All anti-IgLON5 disease stages contributed to the difference with controls (mean difference stage 1: 22.0%, $P = 0.0159$; stage 2: 21.2%, $P = 0.0717$; stage 3: 20.5%, $P = 0.0056$). No difference was found among stages (Fig. 4C). Thus, even if only few cytoplasmic tau-AT8 deposits can be found in stage 1, the nuclear changes occur as frequently as in higher stages of the disease.

Nuclear crenellations were defined as irregularities of the nuclear circumference and ranged from a slight splitting of the membrane to a severe shrinking of the nucleus [Fig. 4B(v–viii); see also methods for the precise quantification of changes]. Quantification of the nuclear crenellations yielded a similar picture as for invaginations. There was a significant increase in the number of mildly and moderately crenellated nuclei (mean difference of 23.0%, $P = 0.0021$) with a corresponding significant reduction in normal nuclei in anti-IgLON5 disease compared with controls as well as among the different disease stages, with a significantly increased number of mild/moderate crenellations at stage 3 (mean difference: 27.0%, $P = 0.0170$). Stage 1 (mean difference: 20.7%, $P = 0.2224$) and stage 2 (mean difference: 16.8%, $P > 0.999$) also showed an increased fraction of crenellated nuclei compared with controls, but only trends or no statistical significance, respectively, due to the smaller number of cases. The PSP group revealed an increase in mild and moderate crenellations compared with controls as well, albeit at a lower level and not reaching significance (mean difference: 15.3%; $P = 0.2305$). Comparison of anti-IgLON5 disease with PSP did not reveal a significant difference (mean difference: 7.6%, $P > 0.999$; Fig. 4D). Overall, nuclei with severe crenellations were not abundant but were more frequently detected in anti-IgLON5 disease cases than in controls, especially at stage 3 [Supplementary Fig. 4B; see also Supplementary Table 3 for full statistical results of nuclear alterations (available at doi.org/10.5281/zenodo.17486565)].

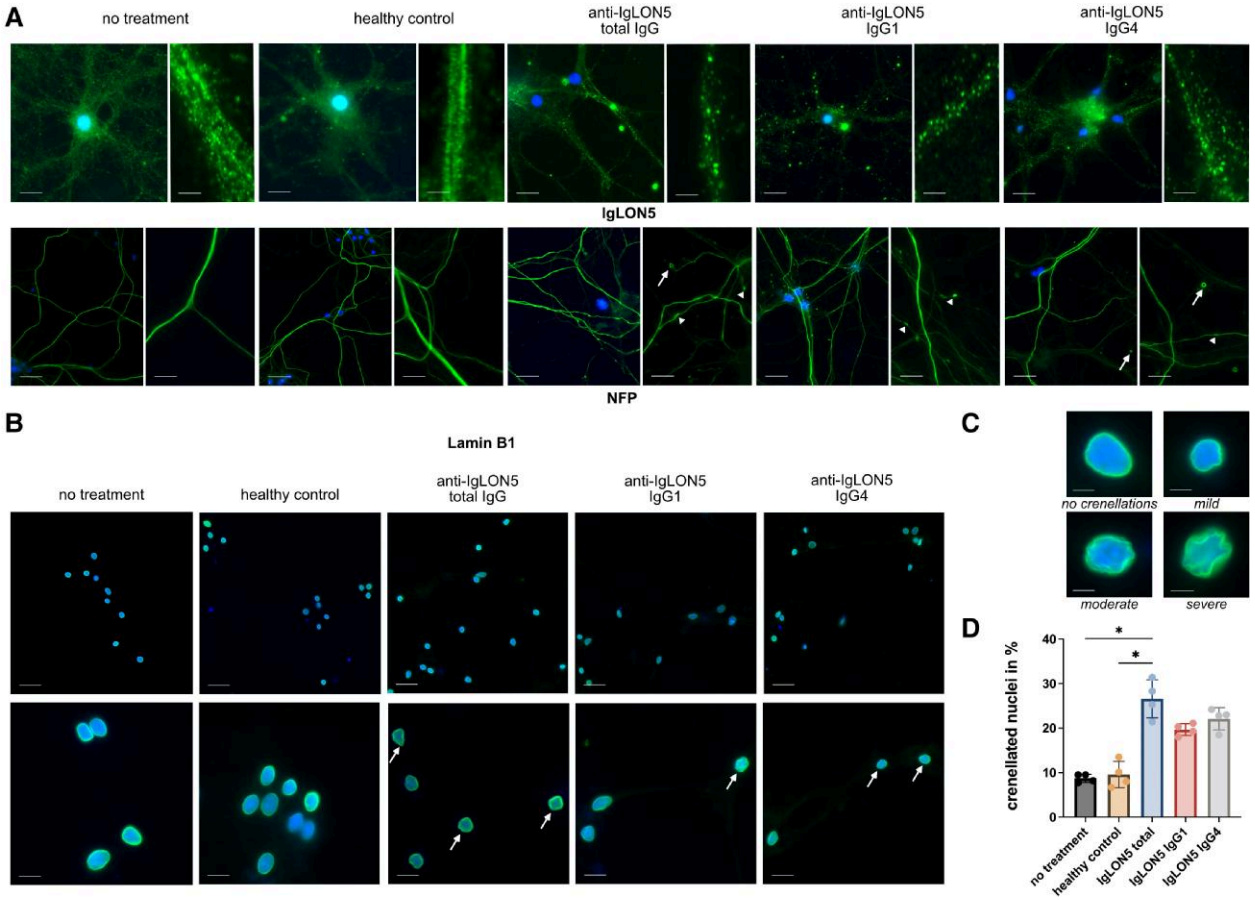

Figure 5 Anti-IgLON5 antibody incubation leads to nuclear membrane crenellations *in vitro*. Rat hippocampal neurons were treated for 3 weeks with anti-IgLON5 total IgG, IgG1- and IgG4-purified human antibodies in parallel to control hippocampal neurons receiving either no treatment or treatment with IgG from a healthy human control. (**A**) Treatment with anti-IgLON5 antibodies leads to reduction of IgLON5 clusters (*top row*) and disruption of neurofilament architecture acquiring ring- and bulb-like morphologies in neurofilament protein (NFP) staining (*bottom row*; arrows indicate example ring-like and arrowheads example bulb-like morphologies). Scale bars: IgLON5 = 20 µm, magnification = 5 µm; NFP = 50 µm, magnification = 10 µm. (**B**) Staining for Lamin B1 reveals shrinking and nuclear membrane alteration with crenellations (arrows) in neurons treated with anti-IgLON5 antibodies. Scale bars = 50 µm (*top row*), 10 µm (*bottom row*). (**C**) Examples of normal and mildly, moderately or severely crenellated neurons in cell culture. Scale bars = 5 µm. (**D**) Quantification of crenellated nuclei (moderate/severe) in per cent of total nuclei in the respective treatment groups, $^{*}P < 0.05$.

Nuclear crenellations also develop *in vitro* after incubation with anti-IgLON5 antibodies

To validate the immunohistochemical observations, we performed an *in vitro* experiment using primary rat hippocampal neurons. Three weeks of incubation with total IgG from anti-IgLON5 disease plasmapheresis material as well as purified anti-IgLON5 IgG1 and anti-IgLON5 IgG4 subclasses showed a significant reduction in the IgLON5 clusters in all three groups compared with the two control groups treated with healthy control IgG and without any antibody treatment, respectively (Fig. 5A). In addition, we observed a significant disruption of the neurofilament architecture in the anti-IgLON5 groups in the neurofilament protein (NFP) staining in the neuronal cultures treated with anti-IgLON5 antibodies. On the one hand, there was a reduction in neurite outgrowth with early termination of dendrites; on the other hand, there were abundant ring- and bulb-like lesions of the nerve cell processes (Fig. 5A). These observations are in line with a previous study by Landa *et al.*[8] and support the pathogenic effect of anti-IgLON5 IgG1/IgG4 antibodies in cell culture.

To test whether the incubation of rat hippocampal neurons with anti-IgLON5 antibodies also led to the nuclear pathology as observed in the post-mortem human tissue samples, we performed an additional staining with anti-Lamin B1 antibodies. In the untreated group and after treatment with healthy control IgG, the neurons predominantly had round-oval nuclei with a smooth, intact nuclear membrane. In contrast, after incubation with anti-IgLON5 antibodies, a fraction of the nuclei appeared significantly smaller and showed alterations of the nuclear membrane with membrane splitting and indentations, analogous to the crenellations observed in the autopsy cases (Fig. 5B). Semi-quantitative assessment of nuclear changes, analogous to the autopsy cases (Fig. 5C), showed a significantly increased proportion of moderate/severe nuclear crenellations after incubation with purified anti-IgLON5 IgG total antibodies compared with the control groups (mean values: no treatment: 8.7%; healthy IgG: 9.6%; IgLON5 total IgG: 26.6%; $P = 0.0125$ and $P = 0.0189$, respectively, Fig. 5D). An increased number of moderate/severe crenellations were also observed after incubation with IgG1- and IgG4-purified anti-IgLON5 antibodies compared with the controls (mean values: IgG1: 19.7%, IgG4: 22.1%), but these were less pronounced than in the anti-IgLON5 IgG total incubation [Fig. 5D; see also Supplementary Table 4 for full statistical results (available at doi.org/10.5281/zenodo.17486565)]. Immunostaining for pTS422

revealed an equivocal, non-specific, diffuse cellular staining pattern that could not be confidently evaluated in relation to an existing specific tau pathology (data not shown).

Discussion

In this study, we characterized the evolution of the disease-associated tauopathy in anti-IgLON5 disease along the different stages of pathology and identified early features of neurodegeneration, providing new insights into the pathophysiology of anti-IgLON5 disease.

A precise characterization of the various pathological PTMs in the development of a tauopathy is crucial for understanding its pathophysiology. While these steps have already been established for other well-characterized tauopathies, they were not previously known for anti-IgLON5 disease. Here, we observed that several PTMs of the tau protein, in particular phosphorylation and acetylation, as detectable by immunohistochemistry, occur during the course of the disease in a particular timeline.

Analogous to two other 3- and 4-repeat tauopathies, namely Alzheimer's disease ('primary' tau pathology) and chronic traumatic encephalopathy (CTE; 'secondary' tau pathology), anti-IgLON5 disease shows a similar pattern of tau PTM (see Table 3 for a detailed comparison).[15-17] In contrast, tau acetylation at K274 occurs late during the course of the disease, which distinguishes it from the 4-repeat tauopathy argyrophilic grain disease (AGD), where this acetylation is not present.[27] Furthermore, in contrast to AGD and to the 3-repeat tauopathy Pick's disease, tau phosphorylation at Ser356/262 is observed.[18,21-26] A clinically and neuropathologically important differential diagnosis of anti-IgLON5 disease is PSP, a 4-repeat tauopathy with similar topographical distribution and overlapping clinical symptoms. The phosphorylation pattern studied here does, however, not differ between the two diseases and is currently not suitable as a singular marker for distinguishing the molecular signature of anti-IgLON5 disease from PSP,[18-20] except for the presence of 3R tau isoforms at later disease stages of most, but not all, anti-IgLON5 disease cases (see Table 3 for a complete overview of the phosphorylation steps of the known tauopathies). Notably, the PSP cases included as a 'positive tauopathy control' in our study also exhibited an increased number of invaginated and crenellated nuclei compared with the controls, although this was less pronounced than in anti-IgLON5 disease and did not reach statistical significance. However, these findings should be corroborated in a larger cohort of PSP cases at different stages of pathology.

While neuronal tau pathology is still the primary feature in anti-IgLON5 disease, most of the cases also show variable glial tau pathology.[4,7] This is mainly represented by mild to moderate oligodendroglial coiled bodies, but also in individual cases of thorn-shaped astrocytes. While the latter might be an age-related component, i.e. ageing-related tau astrogliopathy (ARTAG), it might constitute a further diagnostic challenge to differentiate it from the more common PSP, where a delineation from tufted astrocytes might be sometimes difficult.[28]

Whereas the cellular component of the immune system, including CD8+ T cells, may play a role and contribute to the neurodegenerative process in anti-IgLON5 disease, as shown by the presence of some parenchymal and perivascular T cells in the brain tissue and in close proximity to neurons in an immunological synapse,[6] the antibodies *per se* are sufficient to cause neuronal damage, as observed in cell culture, where nuclear alterations in the form of crenellations are evident after isolated antibody incubation. Furthermore, in contrast to a recent study comparing PSP with Parkinson's disease,[29] we observed no significant differences in the quantification of CD8+ T cells between anti-IgLON5 disease and PSP, indicating that this cellular component cannot be used either to distinguish between the two diseases.

The exact mechanism between antibody binding and the development of a tauopathy remains the subject of intensive research in anti-IgLON5 disease.[2] In this study we were able to provide new insights into the early changes in the disease-associated pathology, showing nuclear alterations as an incipient event in anti-IgLON5 disease. We observed an initial nuclear, and not cytoplasmic, immunoreactivity pattern in the earliest tau phosphorylation step in parallel to early disruptions of the nuclear lamina in the form of invaginations and crenellations as detected by Lamin B1 immunostaining. While the physiological role of tau is seen particularly in the context of modulation of microtubules' dynamics, tau is also localized in the inner nuclear lamina and plays a role in the regulation of the nuclear pore complex.[30-32] Nuclear tau is also involved in the regulation of Lamin B1 expression,[33] and previous studies have shown that a tau-mediated reduction of Lamin B1 can lead to disruptions of the nuclear lamina.[34] Changes in the nuclear lamina are also a characteristic of the normal ageing process,[35] which is reflected in the fact that we detected these changes to a small extent in the age-matched control group as well. However, the anti-IgLON5 disease patients showed a significant increase in the number of affected neurons at all stages of pathology.

The role of nuclear tau in the pathophysiology of tauopathies is an emerging but still understudied topic in neurodegeneration.[36] For instance, prior experimental studies on frontotemporal lobar degeneration (FTLD) by Daude *et al.*[37] using a tau seeding assay featuring a substrate for tau misfolding that comprised a central region of tau with P301L and V337M missense mutations, detected a nuclear membrane staining, reflecting nuclear membrane tau depositions. Moreover, in a study investigating tau exon 10+16 splice site (MAPT IVS10+16)-mutated FTLD autopsy cases as well as iPSC models with IVS10+16 and P301L MAPT mutations, Paonessa *et al.*[38] demonstrated the occurrence of nuclear invaginations, which appear strikingly similar to those observed in the anti-IgLON5 disease cases in our study. In further experiments, the authors found that hyperphosphorylation of tau led to an abnormal projection of microtubules into the nuclear membrane, causing the observed invaginations. The resulting disruption of nucleocytoplasmic transport may thus be an important pathological process in the development of the tauopathy.[38] Whether a similar process might also play a role in anti-IgLON5 disease remains to be elucidated.

Our cell culture experiments confirmed prior results of an antibody-induced reduction in IgLON5 clusters and damage to the neuronal cytoskeleton, thus supporting a direct pathogenic effect of the antibodies.[8,10] Of note, a reduction of IgLON5 clusters was also observed in neuronal cultures incubated with the IgG4 subclass, likely due to the imperfect IgG4 purification and reflecting an effect of the coexisting IgG1 fraction.[10] Incubation with anti-IgLON5 antibodies for 3 weeks also led to a nuclear pathology with alterations of the nuclear membrane in the form of crenellations, as we had observed in post-mortem human brain tissues, supporting our findings *in vitro*. Interestingly, nuclear pathology appeared more pronounced when incubating neurons with total IgG compared with IgG1 or IgG4 alone. Whether this indicates a synergistic effect of the combined antibody subclasses on pathology needs to be investigated in further studies, as this observation was only based on a single patient's sample.

The existing evidence of a neuronal nuclear pathology in other tauopathies,[36-38] combined with the fact that we also observed a

higher number of nuclear lamina alterations in our PSP cases compared with controls, suggests that these changes are not a unique feature of anti-IgLON5 disease but may rather represent a common mechanism of various neurodegenerative diseases. The distinguishing characteristic of anti-IgLON5 disease is its aetiological association with an antibody, which renders it a unique condition and an ideal model for research on common mechanisms in neurodegeneration. In this context, experimental models play a particularly important role, including animal models. However, inducing tauopathies in rodent models, while essential, is still difficult.[39] This is also the case for anti-IgLON5 disease, where it has not yet been possible to induce a tau pathology similar to that seen in humans in mouse models through passive antibody transfer.[40-42] These difficulties are also partly reflected in the findings of our study, in which staining for pTS422 in the rat hippocampal neurons yielded only non-specific results. Ideal future experimental scenarios include animal and cellular models and the analysis of fresh, unfixed human brain tissue with in-depth molecular and biochemical characterizations. For instance, compartmental microdissection of neuronal nuclear and cytoplasmic fractions may prove very useful for studying nuclear pathology in this regard.

The temporal and spatial connection between the deposition of IgG4 antibodies along the neuronal surface and the earliest pathological tau phosphorylation step at Ser422 adds more evidence to the hypothesis that an immune-mediated mechanism precedes or triggers neurodegeneration and that the tauopathy is indeed a time- and antibody-dependent phenomenon, i.e. a secondary tauopathy. Applied to clinical practice, these findings also strengthen the concept that antibody-depleting immunotherapy can potentially mitigate or even prevent further neurodegeneration and tau accumulation at an early stage of the disease, thus underlining the importance of early and intensive immunotherapy. In fact, recent data shows that immunotherapy initiated early is associated with a better outcome in affected patients.[12,13] For diagnostic neuropathology, the new findings also offer an opportunity to make a more reliable diagnosis in early anti-IgLON5 disease cases. We therefore suggest that in autopsy cases that do not show tau deposits with the antibody AT8 (i.e. stage 1 cases),[7] the panel should be extended to include the IHC antibodies against IgG4, Lamin B1 and pTauS422, all of which are commercially available.

In summary, with these new findings, we contribute to a better understanding of the pathophysiology of anti-IgLON5 disease, supporting the concept of an immune-mediated, secondary tauopathy with a timeline of post-translational tau modifications, and provide new insights into the early phase of the disease with an initial nuclear pathology preceding tau deposition. These findings may provide a further basis for exploring the link between autoimmunity and neurodegeneration, which is important not only in anti-IgLON5 disease itself but also as a disease model for other neurodegenerative diseases.

Data availability

Data supporting the findings of this study that are not included in the article or the supplementary material are available from the corresponding author upon reasonable request. Supplementry material is available at Zenodo (doi.org/10.5281/zenodo.17486565).

Acknowledgements

We would like to thank Cristina D'Abramo and Erica Christen, representing the Peter Davis Lab at the Feinstein Institute for Medical Research at Northwell Health, for generously providing the antibodies Alz-50, MC1 and PHF-1. We would also like to thank Li Gan at Weill Cornell Medical College for generously contributing the acetylated Tau K274 antibody. We want to thank Katrin Köbl-Shkreli, Ines Lukac, Isabella Paul, Viktoria Stark and Johanna Wachutka for their excellent technical assistance in Vienna. We are thankful to all brain donors and families for their generous contribution to research, as well as all health personnel in care of the patients along their disease.

Funding

This work was supported by the Austrian Science Fund (FWF), project number I6565-B (SYNABSII), the JPcofuND-2 IGNITEMIND and Austrian Research Promotion Agency (FFG), project number FO999920011, the **Marie Sklodowska-Curie Doctoral Networks, Horizon Europe program, IgG4-TREAT consortium**, grant agreement no. 101119457, and the Austrian Society of Neurology (Österreichische Gesellschaft für Neurologie).

Competing interests

R.R., S.N., F.F., C.E., M.G., A.S.S., V.E., I.K., E.B.S., M.B., E.E., J.F., M.G., A.H., B.H., C.J., J.L., P.M., L.M., J.K.P., P.S., A.S., D.Y.H., S.W., L.S., C.G. and E.G. report no competing interests. M.J.T. has received funds for serving on a scientific advisory board of AmGen, UCB, Arialys and ArgenX, received funds from Dioraphte (2001 0403), filed a patent for methods for typing neurologic disorders and cancer, and devices for use therein, received research funds for consultation at Guidepoint Global LLC, an unrestricted research grant from CSL Behring (Interlaken Leadership Award), and an unrestricted research grant from Euroimmun. He was supported by an E-RARE3 grant (UltraAIE, ZonMW), a JPND grant (IgniteMind, ZonMW), EpilepsieNL (project 19–18), ACT MD (ZonMW), PARADE-VIMP (ZonMW), the Erasmus Trustfonds, the ErasmusMC Foundation and ItsME. R.H. reports speaker's honoraria from UCB and BMS. The Medical University of Vienna (Austria; employer of R.H.) receives payment for antibody assays and for antibody validation experiments organized by Euroimmun (Lübeck, Germany).

References

1. Sabater L, Gaig C, Gelpi E, et al. A novel non-rapid-eye movement and rapid-eye-movement parasomnia with sleep breathing disorder associated with antibodies to IgLON5: A case series, characterisation of the antigen, and post-mortem study. *Lancet Neurol*. 2014;13:575-586.
2. Graus F, Sabater L, Gaig C, et al. Anti-IgLON5 disease 10 years later what we know and what we do not know. *Neurol Neuroimmunol Neuroinflamm*. 2024;12:e200353.
3. Grüter T, Möllers FE, Tietz A, et al. Clinical, serological and genetic predictors of response to immunotherapy in anti-IgLON5 disease. *Brain*. 2023;146:600-611.
4. Gelpi E, Höftberger R, Graus F, et al. Neuropathological criteria of anti-IgLON5-related tauopathy. *Acta Neuropathol*. 2016;132:531-543.
5. Erro ME, Sabater L, Martínez L, et al. Anti-IGLON5 disease: A new case without neuropathologic evidence of brainstem tauopathy. *Neurol Neuroimmunol Neuroinflamm*. 2020;7:e651.
6. Berger-Sieczkowski E, Endmayr V, Haider C, et al. Analysis of inflammatory markers and tau deposits in an autopsy series of

nine patients with anti-IgLON5 disease. *Acta Neuropathol*. 2023; 146:631–645.
7. Gelpi E, Reinecke R, Gaig C, et al. Neuropathological spectrum of anti-IgLON5 disease and stages of brainstem tau pathology: Updated neuropathological research criteria of the disease-related tauopathy. *Acta Neuropathol*. 2024;148:53.
8. Landa J, Gaig C, Plagumà J, et al. Effects of IgLON5 antibodies on neuronal cytoskeleton: A link between autoimmunity and neurodegeneration. *Ann Neurol*. 2020;88:1023-1027.
9. Landa J, Serafim AB, Gaig C, et al. Patients' IgLON5 autoantibodies interfere with IgLON5-protein interactions. *Front Immunol*. 2023;14:1151574.
10. Sabater L, Planagumà J, Dalmau J, Graus F. Cellular investigations with human antibodies associated with the anti-IgLON5 syndrome. *J Neuroinflammation*. 2016;13:226.
11. Yogeshwar SM, Muñiz-Castrillo S, Sabater L, et al. HLA-DQB1*05 subtypes and not DRB1*10:01 mediates risk in anti-IgLON5 disease. *Brain*. 2024;147:2579-2592.
12. Grüter T, Gaig C, Crijnen YS, et al. Early treatment with intravenous immunoglobulins and outcomes of patients with anti-IgLON5 disease. *JAMA Neurol*. 2025;82:1040-1047.
13. Koneczny I, Macher S, Hutterer M, et al. HLA dependency and possible clinical relevance of intrathecally synthesized anti-IgLON5 IgG4 in anti-IgLON5 disease. *Front Immunol*. 2024; 15:1376456.
14. Buchhalter JR, Dichter MA. Electrophysiological comparison of pyramidal and stellate nonpyramidal neurons in dissociated cell culture of rat hippocampus. *Brain Res Bull*. 1991;26:333-338.
15. Xia Y, Prokop S, Giasson BI. "Don't Phos Over Tau": Recent developments in clinical biomarkers and therapies targeting tau phosphorylation in Alzheimer's disease and other tauopathies. *Mol Neurodegener*. 2021;16:37.
16. Arena JD, Smith DH, Lee EB, et al. Tau immunophenotypes in chronic traumatic encephalopathy recapitulate those of ageing and Alzheimer's disease. *Brain*. 2020;143:1572-1587.
17. Katsumoto A, Takeuchi H, Tanaka F. Tau pathology in chronic traumatic encephalopathy and Alzheimer's disease: Similarities and differences. *Front Neurol*. 2019;10:980.
18. Guillozet-Bongaarts AL, Glajch KE, Libson EG, et al. Phosphorylation and cleavage of tau in non-AD tauopathies. *Acta Neuropathol*. 2007;113:513-520.
19. Smith ED, Vo Q, Giasson BI, Borchelt DR, Prokop S, Chakrabarty P. Human tauopathy strains defined by phosphorylation in R1-R2 repeat domains of tau. *Acta Neuropathol Commun*. 2023;11:172.
20. Ishizawa K, Ksiezak-Reding H, Davies P, et al. A double-labeling immunohistochemical study of tau exon 10 in Alzheimer's disease, progressive supranuclear palsy and Pick's disease. *Acta Neuropathol*. 2000;100:235-244.
21. Probst A, Tolnay M, Langui D, Goedert M, Spillantini MG. Pick's disease: Hyperphosphorylated tau protein segregates to the somatoaxonal compartment. *Acta Neuropathol*. 1996;92:588-596.
22. Mondragón-Rodríguez S, Mena R, Binder LI, Smith MA, Perry G, García-Sierra F. Conformational changes and cleavage of tau in Pick bodies parallel the early processing of tau found in Alzheimer pathology. *Neuropathol Appl Neurobiol*. 2008;34:62-75.
23. Hartnell IJ, Woodhouse D, Jasper W, et al. Glial reactivity and T cell infiltration in frontotemporal lobar degeneration with tau pathology. *Brain*. 2024;147:590-606.
24. Rábano A, Cuadros R, Calero M, Hernández F, Avila J. Specific profile of tau isoforms in argyrophylic grain disease. *J Exp Neurosci*. 2013;7:51-59.
25. Tolnay M, Spillantini MG, Goedert M, Ulrich J, Langui D, Probst A. Argyrophilic grain disease: Widespread hyperphosphorylation of tau protein in limbic neurons. *Acta Neuropathol*. 1997;93:477-484.
26. Ferrer I, Barrachina M, Tolnay M, et al. Phosphorylated protein kinases associated with neuronal and glial tau deposits in argyrophilic grain disease. *Brain Pathol*. 2003;13:62-78.
27. Grinberg LT, Wang X, Wang C, et al. Argyrophilic grain disease differs from other tauopathies by lacking tau acetylation. *Acta Neuropathol*. 2013;125:581-593.
28. Yoshida M. Astrocytic inclusions in progressive supranuclear palsy and corticobasal degeneration. *Neuropathology*. 2014;34: 555-570.
29. Couto B, Forrest SL, Fearon C, et al. Midbrain cytotoxic T cells as a distinct neuropathological feature of progressive supranuclear palsy. *Brain*. 2025;148:2650-2657.
30. Gil L, Federico C, Pinedo F, et al. Aging dependent effect of nuclear tau. *Brain Res*. 2017;1677:129-137.
31. Eftekharzadeh B, Daigle JG, Kapinos LE, et al. Tau protein disrupts nucleocytoplasmic transport in Alzheimer's disease. *Neuron*. 2018;99:925-940.e7.
32. Gil L, Niño SA, Capdeville G, Jiménez-Capdeville ME. Aging and Alzheimer's disease connection: Nuclear tau and lamin A. *Neurosci Lett*. 2021;749:135741.
33. Frost B. Alzheimer's disease: An acquired neurodegenerative laminopathy. *Nucleus*. 2016;7:275-283.
34. Montalbano M, McAllen S, Sengupta U, et al. Tau oligomers mediate aggregation of RNA-binding proteins Musashi1 and Musashi2 inducing Lamin alteration. *Aging Cell*. 2019;18:e13035.
35. Kristiani L, Kim M, Kim Y. Role of the nuclear lamina in age-associated nuclear reorganization and inflammation. *Cells*. 2020;9:718.
36. Younas N, Saleem T, Younas A, Zerr I. Nuclear face of tau: An inside player in neurodegeneration. *Acta Neuropathol Commun*. 2023;11:196.
37. Daude N, Kim C, Kang SG, et al. Diverse, evolving conformer populations drive distinct phenotypes in frontotemporal lobar degeneration caused by the same MAPT-P301L mutation. *Acta Neuropathol*. 2020;139:1045-1070.
38. Paonessa F, Evans LD, Solanki R, et al. Microtubules deform the nuclear membrane and disrupt nucleocytoplasmic transport in tau-mediated frontotemporal dementia. *Cell Rep*. 2019;26: 582-593.e5.
39. Szegvari E, Holec SAM, Woerman AL. Limitations and applications of rodent models in tauopathy and synucleinopathy research. *J Neurochem*. 2025;169:e70021.
40. Alvente S, Matteoli G, Molina-Porcel L, et al. Pilot study of the effects of chronic intracerebroventricular infusion of human anti-IgLON5 disease antibodies in mice. *Cells*. 2022;11:1024.
41. Ni Y, Feng Y, Shen D, et al. Anti-IgLON5 antibodies cause progressive behavioral and neuropathological changes in mice. *J Neuroinflammation*. 2022;19:140.
42. Gao Y, Li H, Luo H, et al. Purified serum IgG from a patient with anti-IgLON5 antibody cause long-term movement disorders with impaired dopaminergic pathways in mice. *Biomedicines*. 2023;11:2483.